Hybrid exchange-correlation functional determined from thermochemical data and *ab initio* potentials

Philip J. Wilson, Thomas J. Bradley, and David J. Tozer
Department of Chemistry, University of Durham, South Road, Durham, DH1 3LE United Kingdom

(Received 5 July 2001; accepted 30 August 2001)

Multiplicative potentials, appropriate for adding to the non-multiplicative fractional orbital exchange term in the Kohn–Sham equations, are determined from correlated *ab initio* electron densities. The potentials are examined graphically and are used in conjunction with conventional thermochemical data to determine a new hybrid exchange-correlation functional, denoted B97-2. Calculations using B97-2 are compared with those from (a) the B97-1 functional [J. Chem. Phys. **109**, 6264 (1998)], which has the same functional form and fraction of orbital exchange, but was fitted to just thermochemical data; and (b) the widely used B3LYP functional [J. Chem. Phys. **98**, 5648 (1993)]. B97-2 atomization energies are close to those from B97-1; total electronic energies and ionization potentials are less accurate, but remain an improvement over B3LYP. Molecular structures from all three functionals are comparable. Static isotropic polarizabilities improve from B3LYP to B97-1 to B97-2; the B97-2 functional underestimates experimental values, which is consistent with the neglect of zero-point vibrational corrections. NMR shielding constants—determined as the conventional second derivative of the electronic energy—improve from B3LYP to B97-1 to B97-2. Shieldings determined directly from these DFT electron densities using the recently proposed MKS approach [Chem. Phys. Lett. **337**, 341 (2001)] are two to three times more accurate than the conventional shieldings, and exhibit an analogous improvement across the three functionals. Classical reaction barriers for sixteen chemical reactions improve significantly from B3LYP to B97-1 to B97-2. The introduction of multiplicative potentials into semi-empirical hybrid functional development therefore appears beneficial. © *2001 American Institute of Physics.* [DOI: 10.1063/1.1412605]

I. INTRODUCTION

Kohn–Sham density functional theory (DFT) is widely used for electronic structure calculations.[1] The accuracy of a DFT calculation is governed by the quality of the exchange-correlation energy functional, and so, the continued development of improved approximations to this quantity is essential.

One approach for developing new functionals is to choose a flexible mathematical form and determine optimal parameters by fitting to molecular thermochemical quantities, such as total energies and atomization energies. This semi-empirical route has been widely used for both continuum functionals (where there is a well-defined exchange-correlation potential and no integer discontinuity) such as the generalized gradient approximation (GGA) and for hybrid functionals (which are the sum of a continuum functional and a fraction of exact orbital exchange). Examples of functionals determined by fitting to thermochemical data include the 1988 exchange GGA functional of Becke[2] and the B3LYP,[3] B97,[4] and B97-1[5] hybrid functionals. Thermochemical fits have also been used to determine optimal parameters in more advanced functional forms.[6]

A deficiency of thermochemical fits is that they do not explicitly constrain the Kohn–Sham orbitals and eigenvalues to be accurate. To achieve this, the exchange-correlation contribution to the Kohn–Sham equations must be accurate. Consider a general functional, expressed as the sum of a continuum functional $E_{\mathrm{XC}}^{\xi}[\rho_\alpha,\rho_\beta]$ and a fraction ξ of exact orbital exchange

$$E_{\mathrm{XC}}[\rho_\alpha,\rho_\beta]=E_{\mathrm{XC}}^{\xi}[\rho_\alpha,\rho_\beta]-\frac{\xi}{2}\int\int\sum_{\sigma}\frac{|\rho_{\sigma\sigma}^{1}(\mathbf{r},\mathbf{r}')|^2}{|\mathbf{r}-\mathbf{r}'|}d\mathbf{r}\,d\mathbf{r}', \quad (1)$$

where the label ξ in the continuum contribution indicates an implicit dependence on the fraction of orbital exchange, which in turn is expressed in terms of the Kohn–Sham σ-spin one-densities

$$\rho_{\sigma\sigma}^{1}(\mathbf{r},\mathbf{r}')=\sum_{i}^{N_\sigma}\varphi_{i\sigma}(\mathbf{r})\varphi_{i\sigma}(\mathbf{r}'). \quad (2)$$

This functional represents a conventional continuum functional such as a GGA when $\xi=0$, and a typical hybrid functional when $\xi\approx 0.2$. The Kohn–Sham equations associated with this functional can be derived by minimizing the electronic energy with respect to the Kohn–Sham orbitals. The continuum contribution $E_{\mathrm{XC}}^{\xi}[\rho_\alpha,\rho_\beta]$ in Eq. (1) is an explicit functional of the electron density and so its contribution to the Kohn–Sham equations is the multiplicative scalar potential

$$v_{\mathrm{XC},\sigma}^{\xi}(\mathbf{r})=\frac{\delta E_{\mathrm{XC}}^{\xi}[\rho_\alpha,\rho_\beta]}{\delta\rho_\sigma(\mathbf{r})}. \quad (3)$$

By contrast, the exact exchange term is a functional of the Kohn–Sham orbitals, rather than the density, and so its contribution to the Kohn–Sham equations is non-multiplicative, involving the electron interchange operator $P_{\mathbf{rr}'}$ and the one-density (as in Hartree–Fock theory). The Kohn–Sham equations are written

$$\left(h(\mathbf{r}) + v_{\mathrm{J}}(\mathbf{r}) + v^{\xi}_{\mathrm{XC},\sigma}(\mathbf{r}) - \xi \int d\mathbf{r}' \frac{\rho^{1}_{\sigma\sigma}(\mathbf{r},\mathbf{r}')}{|\mathbf{r}-\mathbf{r}'|} P_{\mathbf{rr}'} - \epsilon_{p\sigma} \right) \varphi_{p\sigma}(\mathbf{r}) = 0, \tag{4}$$

where $h(\mathbf{r})$ is the sum of the kinetic energy operator and the external potential and $v_{\mathrm{J}}(\mathbf{r})$ is the Coulomb (Hartree) potential.

We note that the Kohn–Sham equations (4) could be formulated in an alternative, more theoretically appealing manner, in terms of a purely multiplicative exchange-correlation potential. This can be achieved using the optimized effective potential (OEP) approach,[7] which minimizes the energy with respect to the potential. An alternative route is to solve the non-multiplicative equations (4) for the electron density, and then use the constrained search formulation to determine the multiplicative potential associated with that density. We have demonstrated that this latter method, denoted MKS for ''Multiplicative Kohn–Sham'' is particularly attractive for the calculation of NMR shielding constants.[8] However, the OEP and MKS methods are not widely used at present and so, unless otherwise stated, we use the conventional definition of the Kohn–Sham equations (4) for the present study. Within this formalism, the quality of the Kohn–Sham orbitals and eigenvalues is completely governed by the quality of the multiplicative potential $v^{\xi}_{\mathrm{XC},\sigma}(\mathbf{r})$ for any ξ.

For GGA functionals, $\xi=0$ and $v^{\xi}_{\mathrm{XC},\sigma}(\mathbf{r})$ is the conventional multiplicative exchange-correlation potential. For a GGA to give accurate orbitals and eigenvalues it must therefore provide an accurate representation of the exchange-correlation potential; we have previously attempted to achieve this by explicitly introducing potential information into our fitting procedures. Using the method of Zhao, Morrison, and Parr (ZMP),[9] exchange-correlation potentials have been determined from correlated *ab initio* electron densities for a series of atoms and molecules. The parameters of flexible functional forms have then been optimized such that they yield accurate thermochemistry for the series of molecules, together with exchange-correlation potentials that are maximally parallel to the ZMP potentials. The series of HCTH functionals HCTH/93,[5] HCTH/147,[10] and HCTH/407[11] were determined in this manner and have been successfully applied to molecules resembling those in the fitting data. They can be less successful when applied to systems that differ considerably from those in the fitting data, such as bulk semiconductors involving relatively heavy atoms.[12]

For a hybrid functional ($\xi\neq 0$) to give accurate orbitals and eigenvalues, it, too, must provide an accurate representation of $v^{\xi}_{\mathrm{XC},\sigma}(\mathbf{r})$. However, in this case $v^{\xi}_{\mathrm{XC},\sigma}(\mathbf{r})$ is not the conventional exchange-correlation potential since part of the exchange-correlation contribution to the Kohn–Sham operator is now accounted for in the non-multiplicative orbital exchange term. The conventional ZMP approach takes no account of orbital exchange and so cannot be used to calculate $v^{\xi}_{\mathrm{XC},\sigma}(\mathbf{r})$ from *ab initio* densities. For this reason, multiplicative potential information has not been previously used in the development of semi-empirical hybrid functionals.

In this study the ZMP approach is generalized such that it can be used to calculate $v^{\xi}_{\mathrm{XC},\sigma}(\mathbf{r})$ from *ab initio* densities when $\xi\neq 0$. By analogy with the GGA case, a new hybrid functional is then developed by optimizing its parameters such that it yields accurate thermochemistry for a series of atoms and molecules and has a continuum contribution $E^{\xi}_{\mathrm{XC}}[\rho_\alpha,\rho_\beta]$ whose potential is maximally parallel to the new ZMP potential for these systems. By comparing its performance with that of B97-1, which was determined solely from thermochemical data, the influence of multiplicative potential information in hybrid functional development is quantified. We also take this opportunity to perform a detailed comparison between these highly parameterized functionals and the B3LYP functional, which is widely used in chemical applications.

In Sec. II, a modified ZMP approach is presented for determining $v^{\xi}_{\mathrm{XC},\sigma}(\mathbf{r})$ from *ab initio* densities when $\xi\neq 0$. The potentials for $\xi=0.21$ are presented for Ne, CO, and HF, and are compared with the corresponding exchange-correlation ($\xi=0.0$) and Hartree–Fock-Kohn–Sham correlation ($\xi=1.0$) potentials. In Sec. III, new exchange-correlation functionals are derived for a range of ξ values; an optimal functional is defined by assessing the performance of the functionals for thermochemistry, molecular structures, and six hydrogen abstraction reaction barriers. In Sec. IV, the performance of the new functional is investigated for a range of molecular structures, electric and magnetic response properties, and sixteen chemical reaction barriers. Conclusions are presented in Sec. V.

II. DETERMINATION OF $v^{\xi}_{\mathrm{XC},\sigma}(\mathbf{r})$ FROM THE DENSITY

The ZMP approach is now generalized so it can be applied to functionals of the general form (1). The total electronic energy is

$$E = T_{\mathrm{s}}[\{\varphi_i\}] + E_{\mathrm{ext}}[\rho] + E_{\mathrm{J}}[\rho] + E^{\xi}_{\mathrm{XC}}[\rho_\alpha,\rho_\beta] - \frac{\xi}{2}\int\int \sum_{\sigma} \frac{|\rho^{1}_{\sigma\sigma}(\mathbf{r},\mathbf{r}')|^2}{|\mathbf{r}-\mathbf{r}'|} d\mathbf{r}d\mathbf{r}', \tag{5}$$

where $T_{\mathrm{s}}[\{\varphi_i\}]$, $E_{\mathrm{ext}}[\rho]$, and $E_{\mathrm{J}}[\rho]$ are the non-interacting kinetic energy, the interaction energy between the electrons and the external potential, and the Coulomb (Hartree) energy, respectively.

The energy contributions $E_{\mathrm{ext}}[\rho]$, $E_{\mathrm{J}}[\rho]$, and $E^{\xi}_{\mathrm{XC}}[\rho_\alpha,\rho_\beta]$ are explicit functionals of the spin densities. It follows that if the orbitals are varied subject to the constraint that they yield some reference spin densities, then these terms will remain constant. From the constrained search

formulation,[13] it follows that the Kohn–Sham orbitals associated with the reference densities $\rho_{\alpha 0}$ and $\rho_{\beta 0}$ are obtained through the minimization

$$\min\left(T_s[\{\varphi_i\}] - \frac{\xi}{2}\int\int \sum_\sigma \frac{|\rho^1_{\sigma\sigma}(\mathbf{r},\mathbf{r}')|^2}{|\mathbf{r}-\mathbf{r}'|} d\mathbf{r}d\mathbf{r}' \right) \tag{6}$$

over all sets of orbitals that yield the reference densities. Following ZMP, the constraint is enforced through a Lagrange multiplier λ associated with the self-repulsion condition

$$\int\int \frac{[\rho_\sigma(\mathbf{r})-\rho_{\sigma 0}(\mathbf{r})][\rho_\sigma(\mathbf{r}')-\rho_{\sigma 0}(\mathbf{r}')]}{|\mathbf{r}-\mathbf{r}'|} d\mathbf{r}d\mathbf{r}' = 0 \tag{7}$$

and the equations are brought into the standard Kohn–Sham form by adding $E_{\mathrm{ext}}[\rho]$ to the minimization in Eq. (6). Furthermore, given that the long-range behavior of $v^{\xi}_{\mathrm{XC},\sigma}(\mathbf{r})$ is

$$\lim_{r\to\infty} v^{\xi}_{\mathrm{XC},\sigma}(\mathbf{r}) = \frac{(\xi-1)}{r} + c, \tag{8}$$

additional Fermi–Amaldi-type[14] terms are added to the minimization to impose this behavior. The addition of both extra terms does not affect the minimization since they are explicit functionals of the spin densities. Minimization therefore gives the one-electron equations

$$\left(h(\mathbf{r}) + v^{\lambda}_{\mathrm{J}}(\mathbf{r}) + v^{\lambda}_{\mathrm{J}\sigma}(\mathbf{r})\frac{\xi-1}{N_\sigma} + v^{\lambda}_{\mathrm{C}\sigma}(\mathbf{r}) - \xi\int d\mathbf{r}'\, \frac{\rho^{1\lambda}_{\sigma\sigma}(\mathbf{r},\mathbf{r}')}{|\mathbf{r}-\mathbf{r}'|} P_{\mathbf{r}\mathbf{r}'} - \epsilon^{\lambda}_{p\sigma} \right) \varphi^{\lambda}_{p\sigma}(\mathbf{r}) = 0, \tag{9}$$

where the superscript λ indicates a dependence on the Lagrange multiplier and $v^{\lambda}_{\mathrm{C}\sigma}(\mathbf{r})$ is the σ-spin constraint potential

$$v^{\lambda}_{\mathrm{C}\sigma}(\mathbf{r}) = 2\lambda \int \frac{\rho^{\lambda}_{\sigma}(\mathbf{r}') - \rho_{\sigma 0}(\mathbf{r}')}{|\mathbf{r}-\mathbf{r}'|} d\mathbf{r}'. \tag{10}$$

The equations (9) can be identified as the Kohn–Sham equations associated with the reference densities when the constraint (7) is satisfied. This occurs when $\lambda\to\infty$ and so comparing Eq. (9) in this limit with Eq. (4) leads us to define the potential

$$v^{\xi}_{\mathrm{ZMP},\sigma}(\mathbf{r}) = \lim_{\lambda\to\infty}\left(v^{\lambda}_{\mathrm{J}\sigma}(\mathbf{r})\frac{\xi-1}{N_\sigma} + v^{\lambda}_{\mathrm{C}\sigma}(\mathbf{r}) \right). \tag{11}$$

For a given reference density, this ''ZMP potential'' is the exact asymptotically vanishing multiplicative potential that must be added to ξ times the non-multiplicative orbital exchange term in the Kohn–Sham equations. Note that $v^{\xi}_{\mathrm{ZMP},\sigma}(\mathbf{r})$ and the potential $v^{\xi}_{\mathrm{XC},\sigma}(\mathbf{r})$ in Eq. (4) are not necessarily the same, as they can differ by an additive constant.

A. $v^{\xi}_{\mathrm{ZMP},\sigma}(\mathbf{r})$ for Ne, CO, and HF

Our Gaussian basis set implementation of the ZMP approach has been amended to account for the presence of orbital exchange, as detailed in the previous section. The most successful hybrid functionals include a fraction of orbital exchange $\xi\approx 0.2$ (eg., B3LYP, $\xi=0.2$; B97, $\xi=0.1943$; B97-1, $\xi=0.21$) and so it is informative to ex-

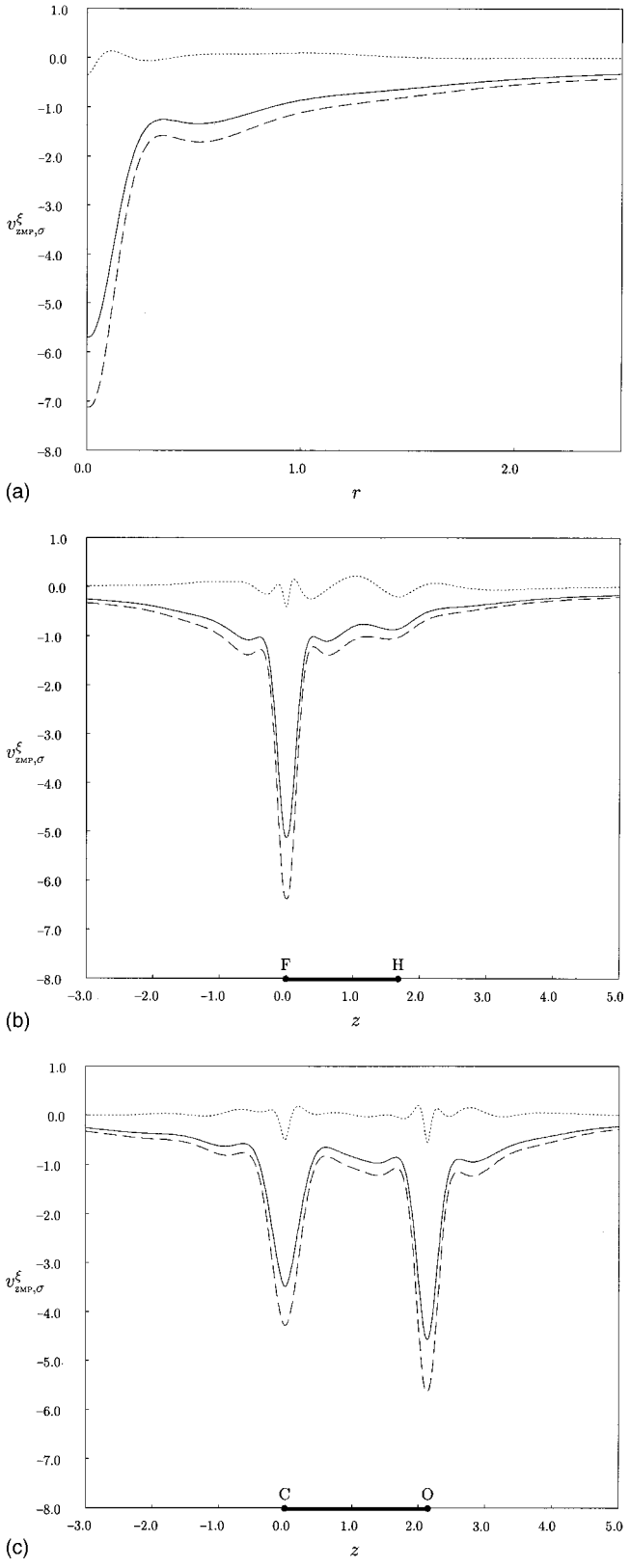

FIG. 1. Multiplicative potentials $v^{\xi}_{\mathrm{ZMP},\sigma}(\mathbf{r})$ with $\xi=1.0$ (dotted lines), $\xi=0.21$ (solid lines), and $\xi=0.0$ (dashed lines) for (a) Ne, (b) HF, and (c) CO. All quantities are in au.

TABLE I. Fitting data used in functional determination:

1. M: H_2, LiH, BeH, CH, $CH_2(^1A)$, $CH_2(^3B)$, CH_3, CH_4, NH, NH_2, NH_3, OH, H_2O, HF, Li_2, LiF, C_2H_2, C_2H_4, C_2H_6, CN, HCN, CO, HCO, H_2CO, CH_3OH, N_2, N_2H_4, O_2, H_2O_2, F_2, CO_2, $SiH_2(^1A)$, $SiH_2(^3B)$, SiH_3, SiH_4, PH_2, PH_3, HCl, Na_2, Si_2, P_2, S_2, Cl_2, NaCl, SiO, CS, SO, ClO, ClF, CH_3Cl, CH_3SH, HOCl, SO_2, HF^+, HCl^+, CO^+, N_2^+, O_2^+, P_2^+, S_2^+, Cl_2^+ {61}
2. A_1: H, He, Li, Be, B, C, N, O, F, Ne {10}
3. A_1^+: Li^+, Be^+, B^+, C^+, N^+, O^+, F^+, Ne^+ {8}
4. A_2: Na, Mg, Al, Si, P, S, Cl {7}
5. A_2^+: Na^+, Mg^+, Al^+, Si^+, P^+, S^+, Cl^+ {7}

amine graphically $v^{\xi}_{\mathrm{ZMP},\sigma}(\mathbf{r})$ for such values. Following the B97-1 functional, $\xi=0.21$ is chosen.

In Figs. 1(a)–1(c) multiplicative potentials $v^{\xi}_{\mathrm{ZMP},\sigma}(\mathbf{r})$, determined for $\xi=0.21$, are presented for Ne, HF, and CO. The α and β potentials are identical as the molecules are closed-shell singlets. For Ne the potential is plotted as a function of radial distance; for the diatomics it is plotted along the bond axis. The potentials were determined from Brueckner Doubles (BD) electron densities using a TZ2P basis set[15] and a Lagrange multiplier $\lambda=900$. (The use of a finite Gaussian basis set makes the limit $\lambda\to\infty$ inappropriate and studies have demonstrated that $\lambda=900$ is acceptable.[16]) For comparison, the conventional exchange-correlation potentials [$v^{\xi}_{\mathrm{ZMP},\sigma}(\mathbf{r})$ when $\xi=0.0$] and the correlation potential of Hartree–Fock-Kohn–Sham theory [$v^{\xi}_{\mathrm{ZMP},\sigma}(\mathbf{r})$ when $\xi=1.0$] are also presented. The correlation potentials for Ne, CO, N_2, and F_2 were presented in a previous study.[17]

The $\xi=0.21$ potentials are intermediate between those of $\xi=0.0$ and $\xi=1.0$. Given that the fraction of orbital exchange is relatively small, they more closely resemble the $\xi=0.0$ potentials, exhibiting similar structural characteristics. In addition to these systems, the H_2, N_2, and F_2 potentials have also been investigated. For all these systems, the $\xi=0.21$ potentials are reasonably well-approximated by

$$v^{\xi}_{\mathrm{ZMP},\sigma}(\mathbf{r})\big|_{\xi=0.21}\approx(1-0.21)v^{\xi}_{\mathrm{ZMP},\sigma}(\mathbf{r})\big|_{\xi=0.0}, \tag{12}$$

although this approximation is not used in our functional development.

III. A NEW HYBRID FUNCTIONAL

In a previous study,[5] we determined the B97-1 hybrid exchange-correlation functional by reoptimizing the B97 functional form of Becke.[4] B97-1 is of the form (1), with $\xi=0.21$ and a continuum part expressed in terms of 9 parameters $\{c_i\}$. Optimal parameters were determined by fitting to thermochemical data only, through the minimization

$$\frac{\partial\Omega_{\mathrm{E}}}{\partial c_i}=0, \tag{13}$$

where Ω_{E} is a measure of thermochemical accuracy

$$\Omega_{\mathrm{E}}=\sum_{\mathrm{T}}^{86}[E_{\mathrm{T}}^{\mathrm{calc}}-E_{\mathrm{T}}^{\mathrm{expt}}]^2. \tag{14}$$

Using the notation in Table I, the 86 energy contributions to Ω_{E} are (a) total energies of first-row atoms A_1 and cations A_1^+; (b) ionization potentials of second-row atoms A_2; and (c) atomization energies of molecules M.

In this study we continue to use the B97-1 functional form and fitting data from Table I, but we now derive the optimal parameters such that the new functional yields accurate thermochemistry *and* has a continuum part $E^{\xi}_{\mathrm{XC}}[\rho_\alpha,\rho_\beta]$ whose potential is maximally parallel to the new ZMP potentials for the systems in the fitting data. For the 93 systems in Table I, multiplicative potentials $v^{\xi}_{\mathrm{ZMP},\sigma}(\mathbf{r})$ were calculated for ξ values of 0.19, 0.20, 0.21, and 0.22, using the TZ2P basis set, $\lambda=900$, and coupled cluster BD or MP2 densities, for closed- and open-shell systems, respectively. When constraining potentials in functional development, it is only necessary for the calculated potentials to be maximally parallel to the ZMP potentials. A possible shift between the two potentials must be introduced because the continuum part of the new functional gives a potential that does not exhibit any integer discontinuity. Following Ref. 18, we define a new quantity, which measures the degree to which the two potentials are parallel

TABLE II. Error assessments for self-consistent molecular structures (Å and degrees), thermochemistry (kcal/mol), and hydrogen abstraction classical reaction barriers (kcal/mol), as a function of the fraction of orbital exchange ξ.

			New functionals			
			ξ			
	B3LYP	B97-1	0.19	0.20	0.21	0.22
Molecular structures						
Mean abs. r	0.008	0.008	0.009	0.008	0.008	0.008
Mean abs. θ	0.2	0.3	0.4	0.3	0.3	0.3
Thermochemistry						
Mean abs. E(A_1, A_1^+)	4.5	2.3	3.3	3.3	3.4	3.4
Mean abs. AE(M)	3.4	1.9	1.9	1.9	2.0	2.0
Mean abs. IP(A_2)	1.8	1.0	1.5	1.4	1.4	1.3
Hydrogen abstraction reaction barriers						
Mean abs.	3.2	3.7	2.6	2.5	2.5	2.5

$$\Omega_{\mathrm{v}}=\sum_{\mathrm{T}}\sum_{\sigma}\int d\mathbf{r}[v^{\xi}_{\mathrm{ZMP},\sigma\mathrm{T}}(\mathbf{r})+k^{\xi}_{\sigma\mathrm{T}} - v^{\xi}_{\mathrm{fit},\sigma\mathrm{T}}(\mathbf{r})]^2\rho^{2/3}_{\sigma\mathrm{T}}(\mathbf{r}), \quad (15)$$

where T sums over the 93 systems in the fitting data; σ denotes α and β spins; $v^{\xi}_{\mathrm{ZMP},\sigma\mathrm{T}}(\mathbf{r})$ is the new σ-spin ZMP potential for system T; $k^{\xi}_{\sigma\mathrm{T}}$ is the σ-spin shift for system T; $v^{\xi}_{\mathrm{fit},\sigma\mathrm{T}}(\mathbf{r})$ is the σ-spin potential associated with the continuum part of the new functional for system T; and $\rho^{2/3}_{\sigma\mathrm{T}}(\mathbf{r})$ is a spatial weighting function. Initial values are chosen for the shifts $k^{\xi}_{\sigma\mathrm{T}}$ and the quantity

$$\Omega_{\mathrm{E,v}}=\omega_{\mathrm{E}}\Omega_{\mathrm{E}}+\omega_{\mathrm{v}}\Omega_{\mathrm{v}}, \quad (16)$$

is minimized in an iterative fashion with respect to both the variable parameters $\{c_i\}$ and the shifts $\{k^{\xi}_{\sigma\mathrm{T}}\}$, using a system of macro- and microiterations. Following Ref. 5, the weights in Eq. (16) are chosen to be $\omega_{\mathrm{E}}=750$ and $\omega_{\mathrm{v}}=1$. As with B97-1, all calculations in the functional development use the TZ2P basis set, and so all the functionals determined in this study are specifically designed for this basis. Unless otherwise stated, all calculations use TZ2P.

A. Dependence on ξ

Four new functionals, corresponding to $\xi=$ 0.19, 0.20, 0.21, and 0.22, have been determined and implemented in the CADPAC program.[19] To choose an optimal functional, molecular structures, thermochemical quantities, and hydrogen abstraction reaction barriers were computed, and compared with experimental or high-level *ab initio* calculations. This criterion for the optimal functional is arbitrary, other properties could have been considered. However, structures and thermochemistry are particularly important, while reaction barriers are a demanding test of any exchange-correlation functional. The error assessment is presented in Table II.

To assess structural accuracy, the mean absolute bond length and bond angle errors are presented for the 40 small molecules of Table IV. These are a subset of the fitting molecules M, where the experimental structures are accurately known. The quality of bond lengths and bond angles is almost constant over the range of ξ values considered, and is very close to that of conventional B97-1 and B3LYP.

Mean absolute errors for the total energies (E) of systems A_1 and A_1^+; ionization potentials (IP) of systems A_2; and atomization energies (AE) of systems M are presented. As with the molecular structures, thermochemical accuracy varies little with ξ. Total energies and ionization potentials are slightly less accurate than B97-1, by approximately 1.0 and 0.4 kcal/mol, respectively. Atomization energies from the new functionals are close to those from B97-1. The new functionals and B97-1 are a significant improvement over B3LYP.

Finally, mean absolute errors for six classical reaction barriers are presented. These reactions were studied previously by Skokov and Wheeler[20] and Hamprecht *et al.*,[5] and correspond to the first six reactions of Table IX. Where more than one *ab initio* value is presented in Table IX, an average value is used for the error analysis. Once again, the variation with ξ is small. Mean absolute errors for the new functionals are a notable improvement over B97-1 and B3LYP.

TABLE III. Functional parameters defining B97-2. See Ref. 5 for definitions of the expansion parameters.

	B97-2
$c_{X\sigma,0}$	+0.827 642D+00
$c_{C\sigma\sigma,0}$	+0.585 808D+00
$c_{C\alpha\beta,0}$	+0.999 849D+00
$c_{X\sigma,1}$	+0.478 400D−01
$c_{C\sigma\sigma,1}$	−0.691 682D+00
$c_{C\alpha\beta,1}$	+0.140 626D+01
$c_{X\sigma,2}$	+0.176 125D+01
$c_{C\sigma\sigma,2}$	+0.394 796D+00
$c_{C\alpha\beta,2}$	−0.744 060D+01
ξ	+0.210 000D+00

It is clear that the variation with ξ is relatively small and that no single value is optimal for all properties. For the remainder of this study, we shall concentrate on the new functional with $\xi=0.21$, since this value is used in B97-1. We denote the new functional as B97-2, as it is a natural extension of B97-1—the sole difference between the two functionals is that the former is fitted to thermochemistry and potentials, while the latter is fitted to just thermochemistry. By comparing the performance of B97-2 and B97-1, the influence of including multiplicative potential information in hybrid functional development will be quantified.

The parameters defining B97-2 are presented in Table III. The third parameter, the local $\alpha\beta$ correlation prefactor, is particularly close to unity, demonstrating that the uniform gas $\alpha\beta$ correlation limit is approximately satisfied. The corresponding prefactor for the B97-1 functional is 0.955 689.

IV. PERFORMANCE OF B97-2

In this section a detailed assessment of B97-2 is presented for the prediction of molecular structures, electric and magnetic response properties, together with a more extensive range of classical reaction barriers.

A. Molecular structures

In Table IV optimized structures for the 40 small molecules are presented. The quality of the nuclear derivative (and hence the molecular structure) is governed, for a given basis set, by the quality of $v^{\xi}_{\mathrm{XC},\sigma}(\mathbf{r})$. Despite being determined from *ab initio* potentials, B97-2 offers minimal improvement over B97-1. Geometries from B3LYP are also of comparable accuracy.

In Table V, optimized bond lengths are presented for a series of diatomic radicals, which are absent from the fitting data. On average, the B97-2 bond lengths are now an improvement over B97-1, which in turn is a slight improvement over B3LYP.

In Table VI, the structures of FOOF, FNO_2 (C_{2v},) O_3, FO_2, $Cr(CO)_6$ and $Ni(CO)_4$ are presented. The TZ2P basis set is used for the first-row atoms; a (14s13p6d)/[8s7p4d] contraction, obtained by augmenting the basis set of Wachters,[34] is used for the transition metals. In FOOF, FNO_2, and O_3, B97-2 bond lengths are uniformly shorter

TABLE IV. Optimized geometries (in Å and degrees) using B3LYP, B97-1 and B97-2 with the TZ2P basis set.

Molecule	B3LYP	B97-1	B97-2	Expt[a]
H_2	0.740	0.739	0.739	0.741
LiH	1.590	1.595	1.601	1.596
BeH	1.341	1.348	1.353	1.343
CH	1.123	1.127	1.124	1.120
$CH_2(^3B)$	1.077	1.080	1.077	1.078
	135.2	135.1	135.1	136.0
$CH_2(^1A)$	1.110	1.113	1.110	1.110
	101.8	101.4	101.4	101.9
CH_3	1.078	1.080	1.077	1.080
CH_4	1.088	1.090	1.087	1.086
NH	1.041	1.042	1.038	1.036
NH_2	1.027	1.028	1.024	1.024
	103.2	102.8	102.8	103.3
NH_3	1.013	1.014	1.009	1.012
	106.9	106.5	106.5	106.7
OH	0.975	0.973	0.970	0.970
H_2O	0.961	0.960	0.956	0.957
	105.0	104.7	104.7	104.5
HF	0.923	0.920	0.916	0.917
Li_2	2.715	2.729	2.754	2.673
LiF	1.571	1.575	1.578	1.564
C_2H_2	1.196	1.199	1.197	1.203
	1.062	1.064	1.062	1.063
C_2H_4	1.325	1.328	1.324	1.331
	1.082	1.084	1.082	1.081
	121.7	121.7	121.7	121.4
CN	1.162	1.165	1.161	1.172
HCN	1.066	1.068	1.066	1.065
	1.146	1.149	1.146	1.153
CO	1.126	1.128	1.125	1.128
HCO	1.173	1.175	1.171	1.173
	1.123	1.125	1.121	1.123
	124.2	123.9	124.1	124.2
H_2CO	1.200	1.201	1.197	1.203
	1.106	1.108	1.105	1.102
	122.0	122.0	122.0	121.9
N_2	1.092	1.095	1.091	1.098
O_2	1.208	1.208	1.198	1.207
H_2O_2	1.456	1.447	1.435	1.456
	0.966	0.965	0.961	0.966
	100.5	100.5	100.8	100.5
F_2	1.404	1.396	1.387	1.412
CO_2	1.160	1.162	1.158	1.160
HCl	1.282	1.284	1.275	1.275
Na_2	3.043	3.073	3.130	3.079
Si_2	2.272	2.273	2.258	2.246
P_2	1.893	1.894	1.885	1.893
S_2	1.915	1.919	1.898	1.889
Cl_2	2.032	2.023	2.003	1.988
NaCl	2.371	2.373	2.378	2.361
SiO	1.513	1.513	1.509	1.510
CS	1.535	1.538	1.533	1.535
SO	1.496	1.494	1.488	1.481
ClO	1.595	1.591	1.576	1.570
ClF	1.653	1.647	1.633	1.628
Mean r	0.004	0.005	0.002	
Mean abs. r	0.008	0.008	0.008	
Mean θ	0.0	−0.2	−0.1	
Mean abs. θ	0.2	0.3	0.3	

[a]Reference 21.

TABLE V. Optimized bond lengths (in Å) for diatomic radicals using B3LYP, B97-1 and B97-2 with the TZ2P basis set.

		B3LYP	B97-1	B97-2	Expt[a]
BH^+	$^2\Sigma^+$	1.203	1.210	1.212	1.215
NH^+	$^2\Pi$	1.079	1.078	1.074	1.070
OH^+	$^3\Sigma^-$	1.038	1.035	1.031	1.029
BeF	$^2\Sigma^+$	1.371	1.373	1.374	1.361
BN	$^3\Pi$	1.317	1.324	1.323	1.329[b]
BO	$^2\Sigma^+$	1.201	1.204	1.203	1.205
C_2^+	$^2\Pi_u$	1.317	1.325	1.317	1.301
CF	$^2\Pi$	1.278	1.277	1.274	1.272
NF	$^3\Sigma^-$	1.324	1.320	1.311	1.317
NO	$^2\Pi$	1.147	1.149	1.143	1.151
OF	$^2\Pi$	1.356	1.348	1.338	1.354[c]
F_2^+	$^2\Pi_g$	1.302	1.294	1.284	1.305[d]
Al_2	$^3\Sigma_g^-$	2.512	2.514	2.482	2.466
SiCl	$^2\Pi$	2.095	2.088	2.079	2.058
NS	$^2\Pi$	1.496	1.496	1.491	1.494
PO	$^2\Pi$	1.482	1.482	1.477	1.476
Mean		0.007	0.007	0.001	
Mean abs.		0.012	0.011	0.009	

[a]Reference 22 unless otherwise stated.
[b]Reference 23.
[c]Reference 24.
[d]Reference 25.

than those of B97-1. For all but the OO bond length in FOOF, this leads to an increased error. The FO and OO bond lengths in FOOF and O_3, respectively, are particularly poor with both hybrid functionals. For FO_2, the FO bond length improves slightly from B97-1 to B97-2, although significant underestimation remains; the OO bond length becomes less

TABLE VI. Optimized structures (in Å and degrees) of FOOF, FNO_2, O_3, FO_2, $Cr(CO)_6$ and $Ni(CO)_4$ using B3LYP, B97-1 and B97-2. See text for basis set details.

	B3LYP	B97-1	B97-2	Expt
		FOOF		
r_{FO}	1.531	1.513	1.509	1.575[a]
r_{OO}	1.228	1.236	1.219	1.217[a]
θ_{FOO}	109.3	109.1	109.4	109.5[a]
τ	88.1	87.9	88.1	87.5[a]
		FNO_2		
r_{FN}	1.487	1.470	1.461	1.467[b]
r_{NO}	1.176	1.179	1.170	1.180[b]
θ_{ONO}	136.3	135.8	135.9	136.0[b]
		O_3		
r_{OO}	1.258	1.256	1.244	1.272[c]
θ_{OOO}	118.1	118.1	118.3	116.8[c]
		FO_2		
r_{FO}	1.631	1.603	1.609	1.649[d]
r_{OO}	1.190	1.194	1.181	1.200[d]
θ_{FOO}	111.2	111.2	111.3	111.2[d]
		$Cr(CO)_6$		
r_{CrC}	1.929	1.921	1.907	1.914,[e] 1.916[f]
r_{CO}	1.139	1.141	1.138	1.140,[e] 1.140[f]
		$Ni(CO)_4$		
r_{NiC}	1.848	1.844	1.834	1.838,[g] 1.817[h]
r_{CO}	1.135	1.137	1.134	1.141,[g] 1.127[h]

[a]Reference 26.
[b]Reference 27.
[c]Reference 28.
[d]Reference 29.
[e]Reference 30.
[f]Reference 31.
[g]Reference 32.
[h]Reference 33.

TABLE VII. Static isotropic polarizabilities (in atomic units) using B3LYP, B97-1, B97-2 and BD(T), with the Sadlej basis set.

	B3LYP	B97-1	B97-2	BD(T)	Expt[a]
HF	5.83	5.75	5.68	5.64	5.60
H_2O	9.95	9.81	9.70	9.71	9.64
N_2	11.93	11.84	11.71	11.75	11.74
CO	13.18	13.05	12.96	13.03	13.08[b]
F_2	8.69	8.62	8.53	8.45	8.38
NH_3	14.72	14.54	14.35	14.33	14.56
CO_2	17.31	17.17	16.99	17.56	17.51
CH_4	17.01	16.86	16.64	16.43	17.27
C_2H_4	28.15	27.92	27.56	26.91	27.70
PH_3	31.34	30.99	30.76	30.44	30.93
H_2S	25.25	24.99	24.61	24.67	24.71
SO_2	25.73	25.50	25.26	26.06	25.61
HCl	17.90	17.73	17.42	17.43	17.39
Cl_2	31.16	30.91	30.46	30.71	30.35
Mean (BD(T))	0.36	0.18	−0.04		
Mean abs. (BD(T))	0.44	0.32	0.22		
Mean (Expt)	0.26	0.09	−0.13	−0.10	
Mean abs. (Expt)	0.33	0.22	0.19	0.25	

[a]Reference 35 unless otherwise stated.
[b]Reference 36.

accurate. For these molecules, the B3LYP description can be more accurate. For the two transition metal complexes, similar quality is obtained with B97-1 and B97-2, while B3LYP is less accurate for the metal ligand distances.

B. Static isotropic polarizabilities

In Table VII, static isotropic polarizabilities are presented for a series of small molecules. All calculations were performed at near-experimental geometries,[21,37] using the Sadlej basis set.[38] The B3LYP, B97-1, and B97-2 polarizabilities do not include zero-point vibrational corrections (ZPVC's), and so are not strictly comparable with the experimental values. For several of the molecules in Table VII, Russell and Spackman[39] have calculated ZPVC's, and find that in all cases the correction increases the calculated polarizability by a non-negligible amount. An accurate non-corrected DFT calculation should therefore underestimate the polarizabilities of these systems. To provide a more valid comparison we also present BD(T) polarizabilities, which neglect ZPVC's; these were determined as the numerical (finite-difference) derivative of the BD(T) electric dipole moment, using a static electric field of magnitude 0.001 au.

In moving from B3LYP to B97-1 to B97-2, there is a uniform reduction in the static isotropic polarizabilities, leading to improved agreement with the reference BD(T) values. The mean errors, relative to BD(T), reduce from 0.36 to 0.18 to −0.04 au for B3LYP, B97-1, and B97-2, respectively. The corresponding mean absolute errors reduce from 0.44 to 0.32 to 0.22 au.

Both B97-2 and BD(T) underestimate experimental polarizabilities by an average of 0.13 and 0.10 au, respectively, which is consistent with the neglect of ZPVC's. By contrast, B3LYP and B97-1 overestimate the experimental values by an average of 0.26 and 0.09 au, respectively, and so their errors will increase upon addition of a positive ZPVC.

To assess the frequency dependence of the polarizability, vertical valence excitation energies were determined for N_2, CO, H_2CO, C_2H_4, and C_6H_6 with appropriate basis sets. Valence excitations from B97-1 and B97-2 were very similar, and so the results are not explicitly presented. B97-2 excitations were equal to or slightly larger (by less than 0.1 eV) than those of B97-1. This led to a slight improvement for N_2, CO, and C_2H_4, where valence excitations are underestimated with B97-1. It slightly reduces the accuracy for H_2CO and C_6H_6, where B97-1 overestimates some of the excitation energies.

C. Isotropic NMR shielding constants

In Table VIII, isotropic NMR shielding constants are presented for a series of small first- and second-row molecules. All calculations were performed at the near-experimental geometries discussed in Ref. 8, using the Huzinaga (IGLO IV) basis set.[44,49] The errors are dominated by the ozone molecule and so errors are also presented when ozone is omitted. The columns headed B3LYP, B97-1 and B97-2 are conventional shielding constants (the second derivatives of the corresponding electronic energies) determined in a coupled fashion. Shieldings are very poor for all three functionals, although there is a notable improvement from B3LYP to B97-1 to B97-2.

In a recent study[8] we introduced a new approach for determining NMR shielding constants directly from theoretical electron densities. In the new approach, denoted MKS (for Multiplicative Kohn–Sham), a fully multiplicative exchange-correlation potential is determined from a theoretical electron density using the conventional ($\xi=0$) ZMP approach. The Kohn–Sham orbitals and eigenvalues associated with this potential are then input into the conventional uncoupled Kohn–Sham shielding expression; for full details of the MKS approach, see Ref. 8. The MKS(B3LYP), MKS(B97-1), and MKS(B97-2) values in Table VIII are shieldings determined from B3LYP, B97-1, and B97-2 electron densities, respectively, using the same combination of TZ2P and Huzinaga (IGLO IV) basis sets used in Ref. 8. The results are two to three times more accurate than the respective shieldings determined in the conventional manner. Again, there is an improvement in quality from MKS(B3LYP) to MKS(B97-1) to MKS(B97-2). When all the molecules are considered, the B97-2 mean absolute error is 15.8 ppm, compared to the best *ab initio* error of 11.2 ppm.

D. Classical reaction barriers

The accurate calculation of chemical reaction barriers is a considerable challenge for Kohn–Sham theory. For many reactions, barriers from conventional GGA and hybrid functionals lie significantly below those from high-level *ab initio* correlated methods (e.g., see Refs. 20, 50, 51), although the errors can be reduced by significantly increasing the fraction of orbital exchange (e.g., see Ref. 52) In Table IX, classical reaction barriers (i.e., no zero-point, thermal, or tunnelling contributions) are presented for sixteen simple reactions. The first column indicates the reactants. The second column describes the nature of the transition state, in each case the

TABLE VIII. Isotropic shielding constants (in ppm) using B3LYP, B97-1, B97-2, MKS(B3LYP), MKS(B97-1), and MKS(B97-2), with the Huzinaga (IGLO IV) basis set.

		B3LYP	B97-1	B97-2	MKS (B3LYP)	MKS (B97-1)	MKS (B97-2)	Best *ab initio*	Expt.
HF	F	412.1	412.3	412.5	414.2	414.4	414.4	418.6[a]	419.7[a]
H_2O	O	327.8	328.4	328.3	329.5	330.2	329.8	337.9[a]	357.6[a]
CH_4	C	188.8	190.6	191.3	188.4	189.9	190.7	198.9[a]	198.4[a]
CO	C	−18.4	−13.9	−12.4	−7.3	−2.7	−2.4	5.6[a]	2.8[a]
	O	−81.2	−80.8	−74.1	−52.2	−50.8	−45.4	−52.9[a]	−36.7[a]
N_2	N	−91.7	−87.9	−85.9	−69.2	−65.1	−64.0	−58.1[a]	−59.6[a]
F_2	F	−252.4	−241.6	−243.1	−211.8	−200.7	−202.7	−186.5[a]	−192.8[a]
O′OO′	O′	−1692.5	−1671.3	−1660.4	−1209.5	−1178.8	−1174.1	−1208.2[a]	−1290[a]
	O	−1127.3	−1112.1	−1099.6	−812.1	−790.5	−782.9	−754.6[a]	−724[a]
PN	P	−54.8	−36.4	−36.3	18.2	37.4	37.1	86[b]	53[b]
	N	−425.8	−419.9	−408.4	−355.9	−348.0	−340.8	−341[b]	−349[b]
H_2S	S	707.5	716.8	722.5	711.9	721.3	725.6	754.6[c]	752[c]
NH_3	N	259.7	260.9	260.9	260.4	261.6	261.3	270.7[a]	273.3[a]
HCN	C	69.4	72.6	73.4	74.9	78.0	78.3	86.3[a]	82.1[a]
	N	−49.3	−45.7	−39.8	−30.7	−27.0	−22.2	−13.6[a]	−20.4[a]
C_2H_2	C	107.1	109.5	111.7	109.9	112.1	113.9	121.8[d]	117.2[e]
C_2H_4	C	47.3	51.0	53.8	51.3	54.8	57.2	71.2[f]	64.5[f]
H_2CO	C	−24.3	−19.4	−16.6	−19.3	−14.7	−12.5	4.7[a]	−4.4[a]
	O	−452.4	−441.9	−424.9	−372.8	−360.6	−348.3	−383.1[a]	−375[a]
N′NO	N′	81.9	85.5	86.7	95.2	98.9	99.7	100.5[g]	99.5[g]
	N	−10.8	−7.1	−2.4	2.4	6.1	10.5	5.3[g]	11.3[g]
	O	173.4	174.0	173.9	188.7	190.1	189.9	198.8[g]	200.5[g]
CO_2	C	49.8	53.9	55.1	53.9	57.9	58.7	63.5[f]	58.8[f]
	O	213.8	214.4	215.7	223.2	224.2	225.2	236.4[h]	243.4[h]
OF_2	O	−583.7	−561.3	−556.0	−526.6	−505.0	−502.1	−465.5[h]	−473.1[h]
H_2CNN'	C	160.2	162.4	162.7	161.3	163.4	163.6	171.9[a]	164.5[a]
	N	−59.8	−53.9	−50.0	−52.5	−46.8	−43.4	−31.6[a]	−43.4[a]
	N′	−192.4	−183.6	−180.2	−146.6	−137.5	−135.4	−142.4[a]	−149.0[a]
HCl	Cl	945.2	949.5	952.4	945.6	949.8	952.0	962.3[i]	952[i]
SO_2	S	−249.4	−226.9	−227.5	−195.3	−172.4	−172.4	−134.2[c]	−126[c]
	O	−282.9	−278.4	−273.8	−224.0	−217.1	−214.7	−170.4[c]	−205[c]
PH_3	P	563.8	576.6	580.0	564.7	577.2	580.4	594[b]	599.9[i]
Mean		−60.7	−53.9	−50.4	−15.4	−7.9	−5.5	4.5	
Mean abs.		60.7	53.9	50.4	20.8	16.5	15.8	11.2	
Mean abs%		76.8	62.6	54.9	36.8	23.2	18.5	19.5	
O_3 omitted									
Mean		−37.9	−31.9	−28.9	−16.2	−9.9	−7.8	3.1	
Mean abs		37.9	31.9	28.9	16.5	11.7	11.1	8.2	

[a]Reference 40, GIAO-CCSD(T), experimental values include rovibrational corrections (except HCN).
[b]Reference 41, SOLO.
[c]Reference 42, IGLO-CASSCF.
[d]Reference 43, GIAO-CCSD.
[e]Reference 44.
[f]Reference 45, GIAO-MP2.
[g]Reference 46, GIAO-CCSD.
[h]Reference 47, GIAO-MP2.
[i]Reference 48, GIAO-MP3.

horizontal dash represents the new bond formed. The next three columns are classical reaction barriers determined using B3LYP, B97-1, and B97-2 with the TZ2P basis set. Barriers were determined using the corresponding DFT optimized structures (details of the structures and electronic symmetries can be found in the *ab initio* references). For all but the final reaction, a transition state was verified by the presence of a single imaginary harmonic vibrational frequency with all three functionals. For the final reaction (constrained to $D_{\infty h}$ symmetry) the energy surface for the bending motion was found to be very flat with all three functionals. In moving from B3LYP to B97-1 to B97-2, there was an increased tendency towards a slightly non-linear transition state with this basis set. For reference, the final column presents classical barriers determined using high-level *ab initio* methods. For the reactions where more than one *ab initio* result is presented, the average value is used in the error analysis.

Although B3LYP provides a more accurate average description than B97-1 for the first six reactions, when all sixteen reactions are considered B97-1 is on average the more accurate functional. Both B3LYP and B97-1 consistently underestimate the reaction barriers, with mean absolute errors of 5.0 and 3.6 kcal/mol, respectively. For the reaction H+NO, B3LYP fails to predict a barrier; this is remedied

TABLE IX. Classical reaction barriers (in kcal/mol) using B3LYP, B97-1 and B97-2, with the TZ2P basis set.

Reaction	TS	B3LYP	B97-1	B97-2	*Ab initio*
$H+H_2$	$H-H_2$	4.01	8.77	9.68	9.61[a]
CH_4+CH_3	H_3CH-CH_3	15.92	13.11	14.47	17.5,[b]16.6[c]
H_2+CH_3	$HH-CH_3$	9.78	8.04	9.15	11.81[d]
H_2+NH_2	$HH-NH_2$	6.33	5.05	6.28	9.51[d]
H_2+OH	$HH-OH$	1.23	0.67	1.90	5.62,[d]4.87[c]
CH_4+OH	H_3CH-OH	2.58	1.30	2.68	6.62,[e]5.11[c]
$H+N_2$	$H-N_2$	7.64	11.62	12.76	15.2,[f]14.5[g]
$N+O_2$	$N-O_2$	6.01	5.51	7.92	8.8,[h]10.2[i]
O+HCl	O−HCl	1.87	0.84	2.98	9.78,[j]10.4[k]
$H+N_2O$	$H-N_2O$	4.94	8.93	10.36	9.6[l]
$H+N_2O$	NNOH	11.84	12.64	16.91	14.5[l]
$H+N_2O$	$H-ON_2$	11.93	16.49	18.75	17.5[l]
H+NO	H−NO	⋯	2.46	3.73	4.1[m]
$O+H_2$	$O-H_2$	6.81	6.91	8.90	12.4[n]
H+HF	H−FH	32.99	40.27	42.48	42.17,[c]46.11[o]
H+HCl	H−ClH	12.40	16.40	18.23	20.72[o]
Mean		−5.0	−3.6	−1.8	
Mean abs.		5.0	3.6	2.4	

[a]Reference 53 QMC.
[b]Reference 54 CI.
[c]Reference 55 CBS-QCI/APNO-0.15.
[d]Reference 56 CCSD(T).
[e]Reference 57 QCISD(T).
[f]Reference 58 CASSCF/CCI.
[g]Reference 59 CCSD(T).
[h]Reference 60 MR-CI.
[i]Reference 61.
[j]Reference 62 MR-CI+Q.
[k]Reference 63 G2Q.
[l]Reference 64 CASSCF/CCI.
[m]Reference 65 CASSCF/CCI.
[n]Reference 66 MR-SDCI.
[o]Reference 50 CCSD(T).

with B97-1, although the barrier remains well below the *ab initio* value.

For every reaction, B97-2 predicts a larger barrier than B97-1; for several of them, B97-2 barriers lie slightly above the *ab initio* values. The mean and mean absolute B97-2 errors of −1.8 and 2.4 kcal/mol, respectively, are a significant improvement over both B3LYP and B97-1. However, significant errors remain, most notably for the reactions H_2+OH, CH_4+OH, and O+HCl. We note that our DFT calculations do not include a BSSE counterpoise correction. Such a correction would further increase the DFT barriers, although a previous study suggests that the correction is small for the TZ2P basis set.[67]

V. CONCLUSIONS

The procedure of Zhao, Morrison, and Parr,[9] which determines multiplicative Kohn–Sham potentials from theoretical electron densities, has been generalized to account for a fraction of exact orbital exchange. Multiplicative potentials, appropriate for adding to 0.21 times the non-multiplicative orbital exchange term in the Kohn–Sham equations, have been examined graphically for Ne, HF, and CO. They show similar structural characteristics to the full exchange-correlation potential. By fitting to thermochemical data and ZMP potentials, a new hybrid exchange-correlation functional, B97-2, has been determined. (The source code for implementation of this functional is available from D.J.Tozer@durham.ac.uk.) For the systems investigated, the performance of B97-2 relative to B97-1 and B3LYP can be summarized as follows:

(a) B97-2 atomization energies are comparable to those from B97-1, while total energies and ionization potentials are slightly less accurate. This reduction in accuracy is unsurprising, given that the emphasis in the fit has been shifted from pure thermochemistry to both thermochemistry and potentials. B97-2 and B97-1 are a significant improvement over B3LYP in these thermochemical studies;

(b) B97-2, B97-1 and B3LYP exhibit similar overall accuracy for molecular structures;

(c) Relative to BD(T), static isotropic polarizabilities improve from B3LYP to B97-1 to B97-2; the latter functional gives polarizabilities that are on average below experimental values, which is consistent with the neglect of vibrational corrections;

(d) Shielding constants determined using two different approaches improve from B3LYP to B97-1 to B97-2. The shieldings determined directly from the DFT densities using the MKS approach are two to three times more accurate than conventional shieldings, determined as the second derivative of the electronic energy; and

(e) Classical reaction barriers improve significantly from B3LYP to B97-1 to B97-2.

Overall, the results suggest that introducing multiplicative potentials into semi-empirical functional development is beneficial. Further assessment of the performance of B97-2 is now required.

ACKNOWLEDGMENT

Financial support from the EPSRC is gratefully acknowledged.

[1] W. Kohn and L. J. Sham, Phys. Rev. **140**, A1133 (1965).
[2] A. D. Becke, Phys. Rev. A **38**, 3098 (1988).
[3] P. J. Stephens, F. J. Devlin, C. F. Chabalowski, and M. J. Frisch, J. Phys. Chem. **98**, 11623 (1994); A. D. Becke J. Chem. Phys. **98**, 5648 (1993)
[4] A. D. Becke, J. Chem. Phys. **107**, 8554 (1997).
[5] F. A. Hamprecht, A. J. Cohen, D. J. Tozer, and N. C. Handy, J. Chem. Phys. **109**, 6264 (1998).
[6] T. Van Voorhis and G. E. Scuseria, J. Chem. Phys. **109**, 400 (1998).
[7] R. T. Sharp and G. K. Horton, Phys. Rev. **90**, 317 (1953); M. R. Norman and D. D. Koelling, Phys. Rev. B **30**, 5530 (1984).
[8] P. J. Wilson and D. J. Tozer, Chem. Phys. Lett. **337**, 341 (2001).
[9] Q. Zhao, R. C. Morrison, and R. G. Parr, Phys. Rev. A **50**, 2138 (1994).
[10] A. D. Boese, N. L. Doltsinis, N. C. Handy, and M. Sprik, J. Chem. Phys. **112**, 1670 (2000).
[11] A. D. Boese and N. C. Handy, J. Chem. Phys. **114**, 5497 (2001).
[12] P. P. Rushton, S. J. Clark, and D. J. Tozer, Phys. Rev. B **63**, 115206 (2001).
[13] M. Levy and J. P. Perdew, in *Density Functional Methods in Physics*, edited by R. M. Dreizler and J. da Providencia (Plenum, New York, 1985), pp. 11–30.
[14] E. Fermi and E. Amaldi, Mem. R. Acad. Italia. **6**, 117 (1934).
[15] T. H. Dunning, Jr., J. Chem. Phys. **55**, 716 (1971); S. Huzinaga *ibid.*, **42**, 1293 (1965).
[16] D. J. Tozer, V. E. Ingamells, and N. C. Handy, J. Chem. Phys. **105**, 9200 (1996).
[17] G. K-L. Chan, D. J. Tozer, and N. C. Handy, J. Chem. Phys. **107**, 1536 (1997).
[18] D. J. Tozer and N. C. Handy, J. Chem. Phys. **108**, 2545 (1998).
[19] R. D. Amos, I. L. Alberts, J. S. Andrews, *et al.*, CADPAC6.5, The Cambridge Analytic Derivatives Package (1998).
[20] S. Skokov and R. A. Wheeler, Chem. Phys. Lett. **271**, 251 (1997).
[21] N. C. Handy and D. J. Tozer, Mol. Phys. **94**, 707 (1998).
[22] K. P. Huber and G. Herzberg, *Constants of Diatomic Molecules* (Van Nostrand Reinhold, New York, 1979).
[23] H. Bredohl, I. Dubois, Y. Houbrechts, and P. Nzohabonayo, J. Mol. Spectrosc. **112**, 430 (1985).
[24] J. B. Burkholder, P. D. Hammer, C. J. Howard, and A. R. W. McKellar, J. Mol. Spectrosc. **118**, 471 (1986).
[25] R. P. Tuckett, A. R. Dale, D. M. Jaffey, P. S. Jarrett, and T. Kelly, Mol. Phys. **49**, 475 (1983).
[26] R. H. Jackson, J. Chem. Soc. **4585**, (1962); K. C. Kim and G. M. Campbell, J. Mol. Struct. **129**, 263 (1985).
[27] R. R. Smardzewski and W. B. Fox, J. Chem. Phys. **60**, 2980 (1974).
[28] T. Tanaka and Y. Morino, J. Mol. Spectrosc. **33**, 538 (1970); A. Barbe and C. Secroun, *ibid.* **49**, 171 (1974).
[29] C. Yamada and E. Hirota, J. Chem. Phys. **80**, 4694 (1984).
[30] A. Jost, B. Rees, and W. B. Yelon, Acta Crystallogr., Sect. B: Struct. Crystallogr. Cryst. Chem. **31**, 2649 (1975).
[31] B. Rees and A. Mitschler, J. Am. Chem. Soc. **98**, 7918 (1976).
[32] L. Hedberg, T. Iijima, and K. Hedberg, J. Chem. Phys. **70**, 3224 (1979).
[33] D. Braga, F. Grepioni, and A. G. Orpen, Organometallics **12**, 1481 (1993).
[34] A. J. H. Wachters, J. Chem. Phys. **52**, 1033 (1970).
[35] C. V. Caillie and R. D. Amos, Chem. Phys. Lett. **328**, 446 (2000).
[36] M. A. Spackman, J. Chem. Phys. **94**, 1288 (1991).
[37] D. J. Tozer and N. C. Handy, J. Chem. Phys. **109**, 10180 (1998).
[38] A. J. Sadlej, Collect. Czech. Chem. Commun. **53**, 1995 (1988); Theor. Chim. Acta **79**, 123 (1991).
[39] A. J. Russell and M. A. Spackman, Mol. Phys. **84**, 1239 (1995); **90**, 251 (1997).
[40] J. Gauss and J. F. Stanton, J. Chem. Phys. **104**, 2574 (1996).
[41] T. D. Bouman and A. E. Hansen, Chem. Phys. Lett. **175**, 292 (1990).
[42] K. Ruud, T. Helgaker, R. Kobayashi, P. Jørgensen, K. L. Bak, and H. J. A. Jensen, J. Chem. Phys. **100**, 8178 (1994).
[43] J. Gauss and J. F. Stanton, J. Chem. Phys. **103**, 3561 (1995).
[44] W. Kutzelnigg, U. Fleischer, and M. Schlindler, *NMR-Basic Principles and Progress*, (Springer, Heidelberg, 1990), Vol. 23.
[45] J. R. Cheeseman, G. W. Trucks, T. A. Keith, and M. J. Frisch, J. Chem. Phys. **104**, 5497 (1996).
[46] J. Gauss and J. F. Stanton, J. Chem. Phys. **102**, 251 (1995).
[47] J. Gauss, Chem. Phys. Lett. **191**, 614 (1992).
[48] H. Fukui, T. Baba, J. Narumi, H. Inomata, K. Miura, and H. Matsuda, J. Chem. Phys. **105**, 4692 (1996).
[49] S. Huzinaga, *Approximate Atomic Functions* (University of Alberta Press, Edmonton, 1971).
[50] M. Filatov and W. Thiel, Chem. Phys. Lett. **295**, 467 (1998).
[51] J. L. Durant, Chem. Phys. Lett. **256**, 595 (1996).
[52] B. J. Lynch, P. L. Fast, M. Harris, and D. G. Truhlar, J. Phys. Chem. A **104**, 4811 (2000).
[53] Y.-S. M. Wu, A. Kuppermann, and J. B. Anderson, Phys. Chem. Chem. Phys. **1**, 929 (1999).
[54] C. Musgrave, J. K. Perry, R. C. Merkle, and W. A. Goddard III, Nanotechnology **2**, 187 (1991).
[55] D. K. Malick, G. A. Petersson, and J. A. Montgomery, Jr, J. Chem. Phys. **108**, 5704 (1998).
[56] E. Kraka, J. Gauss, and D. Cremer, J. Chem. Phys. **99**, 5306 (1993).
[57] K. D. Dobbs, D. A. Dixon, and A. Komornicki, J. Chem. Phys. **98**, 8852 (1993).
[58] S. P. Walch, J. Chem. Phys. **93**, 2384 (1990).
[59] J. Gu, Y. Xie, and H. F. Schaefer III, J. Chem. Phys. **108**, 8029 (1998).
[60] G. Suzzi Valli, R. Orru, E. Clementi, A. Lagana, and S. Crocchianti, J. Chem. Phys. **102**, 2825 (1995).
[61] S. P. Walch and R. L. Jaffe, J. Chem. Phys. **86**, 6946 (1987).
[62] B. Ramachandran, E. A. Schrader III, J. Senekowitsch, and R. E. Wyatt, J. Chem. Phys. **111**, 3862 (1999).
[63] J. L. Durant and C. M. Rohlfing, J. Chem. Phys. **98**, 8031 (1993).
[64] S. P. Walch, J. Chem. Phys. **98**, 1170 (1993).
[65] S. P. Walch and C. M. Rohlfing, J. Chem. Phys. **91**, 2939 (1989).
[66] S. P. Walch, J. Chem. Phys. **86**, 5670 (1987).
[67] D. J. Tozer and N. C. Handy, J. Phys. Chem. A **102**, 3162 (1998).